



Automatic caries detection in bitewing radiographs—Part II: experimental comparison

Antonín Tichý¹ · Lukáš Kunt² · Valéria Nagyová¹ · Jan Kybic²

Received: 19 September 2023 / Accepted: 23 January 2024
© The Author(s) 2024

Abstract

Objective The objective of this study was to compare the detection of caries in bitewing radiographs by multiple dentists with an automatic method and to evaluate the detection performance in the absence of a reliable ground truth.

Materials and methods Four experts and three novices marked caries using bounding boxes in 100 bitewing radiographs. The same dataset was processed by an automatic object detection deep learning method. All annotators were compared in terms of the number of errors and intersection over union (IoU) using pairwise comparisons, with respect to the consensus standard, and with respect to the annotator of the training dataset of the automatic method.

Results The number of lesions marked by experts in 100 images varied between 241 and 425. Pairwise comparisons showed that the automatic method outperformed all dentists except the original annotator in the mean number of errors, while being among the best in terms of IoU. With respect to a consensus standard, the performance of the automatic method was best in terms of the number of errors and slightly below average in terms of IoU. Compared with the original annotator, the automatic method had the highest IoU and only one expert made fewer errors.

Conclusions The automatic method consistently outperformed novices and performed as well as highly experienced dentists.

Clinical significance The consensus in caries detection between experts is low. An automatic method based on deep learning can improve both the accuracy and repeatability of caries detection, providing a useful second opinion even for very experienced dentists.

Keywords Dental caries detection · Convolutional neural networks · Ground truth · Bitewing · X-ray images

Notation and abbreviations

$ \cdot $	Number of elements in a set	D_1	Test dataset
a, A	Annotator, set of all annotators	e	Number of annotation errors
$b, b \cong b'$	Bounding box, matching boxes	E, E	Expert annotator, set of expert annotators
B	Set of bounding boxes	i	Image
D_0	Training dataset	M	Automatic method
		N	Novice annotators
		S	Consensus standard
		κ	Cohen's kappa coefficient of inter-rater reliability
		Ω	Matching between two sets of bounding boxes
		CNN	Convolutional neural network
		$CVAT$	Computer vision annotation tool
		IoU	Intersection over union
		$R - CNN$	Region-based object detection architecture
		$ResNet$	Residual neural network (architecture)
		$RetinaNet$	CNN object detection architecture
		$Swin$	Shifted windows (transformer architecture)
		$YOLO$	You only look once (object detection architecture)

✉ Jan Kybic
kybic@fel.cvut.cz

Antonín Tichý
antonin.tichy@lf1.cuni.cz

Lukáš Kunt
kunt.lukas@gmail.com

Valéria Nagyová
valeria.nagyova@lf1.cuni.cz

¹ Institute of Dental Medicine, First Faculty of Medicine of the Charles University and General University Hospital in Prague, Prague, Czech Republic

² Faculty of Electrical Engineering, Czech Technical University in Prague, Prague, Czech Republic

Introduction

With more than 3.5 billion people affected, dental caries is the most prevalent disease [1, 2]. While preventive measures are considered as the primary way to decrease the dental care expenses, early caries detection is also important, as it may avoid the need of costly restorative treatment [3]. However, the widely used visual inspection or visual-tactile examination may be insufficient to detect incipient caries [4, 5]. In particular, this applies to the proximal surfaces of posterior teeth, for which radiographs are frequently taken [6].

According to a systematic review and meta-analysis by Schwendicke et al. [7], radiographic caries detection is highly accurate for cavitated lesions and dentin caries. However, lower sensitivity was found for initial lesions, and it was suggested that other complementary methods, such as laser fluorescence, transillumination, or electric conductivity measurement [8], are used in a population with high caries risk and prevalence. The meta-analysis also reported a high variability in accuracy and low-inter observer agreement [7, 9]. The underlying factors of the variability were classified as clinical (e.g., lesion depth, dentition, surface location) and methodological (e.g., clinical vs. in vitro settings, reference standard, the number and experience of examiners) [7]. Some in vitro studies reported high inter- and intra-observer agreement [10, 11]. However, the in vitro assessment is considerably different from clinical in vivo studies. As a result, in vitro studies might overestimate sensitivity and underestimate specificity. They were also reported to be more susceptible to small-study effects or publication bias [7].

Deep learning

It has been suggested that deep learning could assist in overcoming some of the mentioned issues. Convolutional neural networks (CNNs) have been used in various medical applications, including dental caries detection. In many tasks, e.g., classification, detection, or segmentation, the performance of CNNs is comparable or even superior to experts [9, 12]. For caries detection, image datasets are annotated by experts and the labeled data are then used for the training of CNNs which learn to recognize specific features of caries. Provided that the dataset has a sufficient quality and size, CNNs are able to predict caries in unknown images with a high accuracy [9, 12].

The annotation requires a high level of expertise and is very time-consuming. Furthermore, the ground truth should preferably be based on the opinion of multiple experts, as the reference set by a single expert may be biased [9]. On the other hand, if the dataset is annotated by multiple experts, the inter-expert variability may lead to incongruous annotations. This problem may be mitigated by using majority voting, but

in the absence of a solid reference, visual evaluation of the radiographs should not be regarded as fully conclusive.

The reference standard, also called the “gold” standard, may be destructive (histologic, microradiographic or operative assessment) or non-destructive (visual-tactile assessment) [7]. Given the high number of images required for machine learning, destructive methods are not applicable. Therefore, three of the previous studies [13–15] verified the existence of caries clinically but that may have even been counterproductive, given the low sensitivity of proximal caries detection in posterior teeth [5]. The uncertainty led some researchers to use a 5-point scale: 1, caries definitely present; 2, caries probably present; 3, uncertain-unable to tell; 4, caries probably not present; and 5, caries definitely not present [10, 11, 16].

Experimental evaluation

The first objective of this work was to compare the performance of a deep learning-based automatic caries detection method presented in a companion “Part I” paper [17] to 8 human annotators, ranging from novices to experts, and including the original annotator who created the training dataset for the automatic method. The second objective was to address the unavailability of the “gold” standard for reference. Multiple ways of evaluating the performance were used, including pairwise comparisons and creation of a consensus standard. The methods are first described in “Methods” section with most results shown in “Results” section.

Methods

The best performing method from “Part I” [17] was used. It is an ensemble of 4 different types of object detection CNNs: RetinaNet-SwinT, Faster R-CNN-ResNet50, YOLOv5-M and RetinaNet-R101. The automatic method, denoted M , was trained on a dataset D_0 with 3989 anonymized bitewing images [17]. The carious lesions were annotated by tight fitting bounding boxes by an expert E_0 with 5 years of experience (A.T.) The Computer Vision Annotation Tool (CVAT)¹ was used for annotations.

For testing, dataset D_1 containing 100 images was created [18] with no overlap between D_0 and D_1 . As in D_0 [17], the radiographs in D_1 were acquired using four different intraoral X-ray units, three of which used direct radiography and one employed indirect radiography. Sensor physical dimensions ranged from 31×41 mm to 27×54 mm. To simplify processing, all images were rescaled to 896×1024

¹ <https://github.com/opencv/cvat>

pixels, with the wide-sensor images padded with black horizontal margins to preserve the aspect ratio. Bitewings with large overlaps of adjacent proximal surfaces or major artifacts were excluded from D_1 . Bitewings in D_1 presented only permanent teeth, but their inclusion was not limited by the number of displayed teeth, presence or size of caries and presence of restorations.

Besides E_0 , four dentists with more than fifteen years of experience (*experts*, denoted E_1, \dots, E_4) and three dentists with less than five years of experience (*novices*, denoted N_1, N_2, N_3) were recruited. The dentists were given instructions on how to use CVAT and asked to annotate all carious lesions in dataset D_1 regardless of their size using tight fitting boxes. The annotators worked completely independently in order to avoid introducing any bias.

The group of all annotators will be denoted $A = \{E_0, E_1, \dots, E_4, N_1, N_2, N_3, M\}$, including the automatic method M . For each image $i \in D_1$, each annotator $a \in A$ yielded a (possibly empty) set of detections, represented as bounding boxes $B_{ia} = \{b_{ia}^1, b_{ia}^2, \dots\}$. Example annotations of the same image (Fig. 1) show that there were marked differences between annotators in both the size and position of bounding boxes. This was confirmed by the annotation statistics in Table 1 — the number of annotations varied between 241 and 425, and one annotator (E_4) created bounding boxes twice as big as most of the others.

Pairwise comparison

The similarity of the annotations between all pairs of annotators $(a, a') \in A \times A$ was evaluated. For each image i , two sets of bounding boxes, B_{ia} and $B_{ia'}$ were produced, which will be denoted B and B' , respectively.

Two bounding boxes b and b' were considered to correspond to the same lesion if the centroid of one was inside the



Fig. 1 Sample image from D_1 with the annotations of the 8 human annotators. Each color corresponds to one annotator

Table 1 Number of annotations, mean length of rectangle sides and their standard deviation for each annotator on dataset D_1

Annotator	Num	Mean	Std
M	256	47.96	21.95
E_0	269	54.76	25.13
E_1	425	65.37	31.92
E_2	264	50.91	30.34
E_3	294	74.03	32.77
E_4	241	100.11	35.98
N_1	384	56.53	21.92
N_2	366	62.93	24.13
N_3	342	57.88	30.29

other or vice versa

$$b \cong b' \iff \text{centroid}(b) \in b' \vee \text{centroid}(b') \in b \quad (1)$$

Note that this relation is reflexive and symmetric but not transitive.

To evaluate the similarity between the two sets of annotations B and B' , we first found a matching $\Omega \subseteq B \times B'$, such that all pairs $(b, b') \in \Omega$ matched ($b \cong b'$) and each box from B or B' appeared in Ω at most once. The correspondence was usually rather clear, so the following simple greedy algorithm was used:

1. Find the largest box b from $B \cup B'$. Without loss of generality, assume that $b \in B$, otherwise exchange the roles of b and b' .
2. Find a corresponding box $b' \in B'$ such that $b' \cong b$ (see (1)), i.e., the boxes match. If there are multiple such b' , choose the one that maximizes the intersection $|b \cap b'|$. If it is not unique, pick the largest b' .
3. If a match b' was found, insert (b, b') into Ω and remove b from B and b' from B' .
4. Repeat until B or B' is empty or all boxes have been considered.

The *number of errors* for the current image i was then the number of remaining unmatched boxes

$$e_{aa'}^i = e(B, B') = |B| + |B'| \quad (2)$$

Both missed lesions (false negatives) and incorrect detections (false positives) were counted as errors. The total number of errors for two annotators a, a' was the sum over all images

$$e_{aa'} = \sum_{i \in D_1} e_{aa'}^i \quad (3)$$

The number of errors is important, because it indicates the agreement of the annotators on the presence or absence of caries in a certain part of the tooth, irrespective of the pixel-precise location and size of the bounding box that differed widely among annotators. This measure was introduced to evaluate the annotation agreement by other means than the widely used *intersection over union* (IoU), which often reaches low values even when it is clear that the same lesion is annotated.

Mean IoU was subsequently calculated to evaluate the overlap of the matched bounding boxes between two annotators a, a' over the whole dataset as a mean of all matched annotations

$$IoU_{aa'} = \frac{\sum_{i \in D_1} \sum_{(b,b') \in \Omega_i^{aa'}} IoU(b, b')}{\sum_{i \in D_1} |\Omega_i^{aa'}|} \tag{4}$$

where $\Omega_i^{aa'}$ was the identified matching between annotations of a and a' in image i . $IoU_{aa'}$ served to evaluate the localization accuracy, while ignoring unmatched annotations, including completely missed (false negative) or spurious (false positive) annotations. These were only reflected in the number of errors $e_{aa'}$.

Significance of pairwise differences

For the pairwise comparison with experts $\{E_0, E_1, E_2, E_3, E_4\}$, the significance of the differences between annotators a and b in terms of the number of errors e was evaluated by the Wilcoxon signed-rank test applied to the sequence

$$\Delta e_{ab}^i = \sum_{\substack{c \neq a \\ c \neq b}} e(B_{ia}, B_{ic}) - e(B_{ib}, B_{ic}) \tag{5}$$

where the sum was over the experts, $c \in \{E_0, E_1, \dots, E_4\}$. An analogous procedure was performed for the IoU measure. It is noteworthy that the non-expert annotators including M were disadvantaged in these comparisons, as they were not used as a reference. For results, see “[Pairwise comparison](#)” section.

Average number of errors and IoU

The measures $IoU_{aa'}$ and $e_{aa'}$ for a given annotator a were averaged over either experts ($a' \in \{E_0, E_1, E_2, E_3, E_4\}$) or over all other annotators excluding M to evaluate how close each annotator is to the “human average”:

$$IoU_a = \text{mean}_{a' \neq a} IoU_{aa'} \tag{6}$$

$$e_a = \text{mean}_{a' \neq a} e_{aa'} \tag{7}$$

Note that this definition disadvantaged M , which was never included in the mean.

Comparison with a consensus standard

As an alternative to the pairwise evaluation described above, the annotations of the experts $E = \{E_1, E_2, E_3, E_4\}$ were combined into a *consensus standard* S , to be compared with all annotators A . Note that expert E_0 was not included in the consensus standard to avoid bias. To avoid an unfair advantage to the remaining experts, 4 different standards $S_{234}, S_{134}, S_{124}, S_{123}$ were created, in each case excluding the expert being evaluated. Other annotators (E_0, N_1, N_2, N_3, M) were evaluated on these 4 consensus standards and the results averaged.

To create the consensus standard from the expert annotations B_{ia} for an image i and $a \in E$, where E is the set of experts involved, the following greedy algorithm was used, similar to the one in “[Pairwise comparison](#)” section

1. Find the largest box b from all $B_{i\tilde{a}}$, with $\tilde{a} \in E$. Remove b from $B_{i\tilde{a}}$.
2. For each $a' \in E, a' \neq \tilde{a}$, find boxes $b_{a'} \in B_{ia'}$ such that $b_{a'} \cong b$ (1), i.e., the boxes match. Let B' be a set of such boxes $b_{a'}$, possibly empty.
3. Remove all boxes B' from their original sets $B_{ia'}$.
4. If $|B'| + 1 > |E|/2$, take the coordinate-wise mean of the bounding boxes $B' \cup \{b\}$ and add the resulting mean bounding box to the consensus standard S .
5. Otherwise, add b to a minority set S' .
6. Repeat until all B_{ia} are empty.

As a result, the consensus standard S contained lesions marked by the majority of experts (in our case two or three). Other lesions marked by a single expert were considered tentative and included in the minority set S' . Tentative lesions were counted as neither true positive nor false positive detections.

The resulting numbers of annotated lesions in the consensus standard are shown in Table 2. It can be seen that the agreement between experts was again weak, the number of unconfirmed lesions proposed by one of the experts was similar in scale to the number of lesions confirmed by the majority.

Since expert E_1 seemed to annotate very differently from the other experts, having marked almost twice as many lesions (see Table 1), a reduced version of the standards was also created without expert E_1 . In this case, consensus standards were created based on only two experts and both had to agree for a lesion to be included; otherwise, their annotations were considered as tentative.

Table 2 The number of annotated lesions agreed on by the majority of experts and by a single expert (minority) in the consensus standard. See Table 1 for comparison

Consensus standard	Number of annotations	
	Majority S	Minority S'
$S_{2,3,4}$	245	180
$S_{1,3,4}$	275	238
$S_{1,2,4}$	251	306
$S_{1,2,3}$	275	276

For each annotator, IoU and the number of errors e with respect to all applicable consensus standards were calculated and averaged over these standards. For results, see “Comparison with a consensus standard” section.

Comparison with the original annotator

Finally, all annotators were compared with the original annotator E_0 . Note that this may have favored M , which learned from E_0 .

To evaluate statistical significance of the differences between annotators a and b , the Wilcoxon signed-rank test

was applied to the sequence:

$$f_{ab}^i = e(B_{ia}, B_{iE_0}) - e(B_{ib}, B_{iE_0}) \tag{8}$$

and similarly for IoU. For results, see “Comparison with the original annotator” section.

Results

Pairwise comparison

Two measures, $\text{IoU}_{aa'}$ and $e_{aa'}$ (“Pairwise comparison” section), are shown for all pairs of annotators in Fig. 2. It can be seen that the automatic method M was the closest to the original annotator E_0 , and the comparisons of M with E_2 , E_3 , and E_4 are also well within the cloud of other pairwise comparison results, yielding very good results especially in terms of the number of errors e . The numeric values of $\text{IoU}_{aa'}$ and $e_{aa'}$ are presented in Table 3. Even the best matching annotators disagreed on 76 lesions, i.e., almost one false positive or false negative annotation per image. Perhaps surprisingly, two experts could disagree on more than

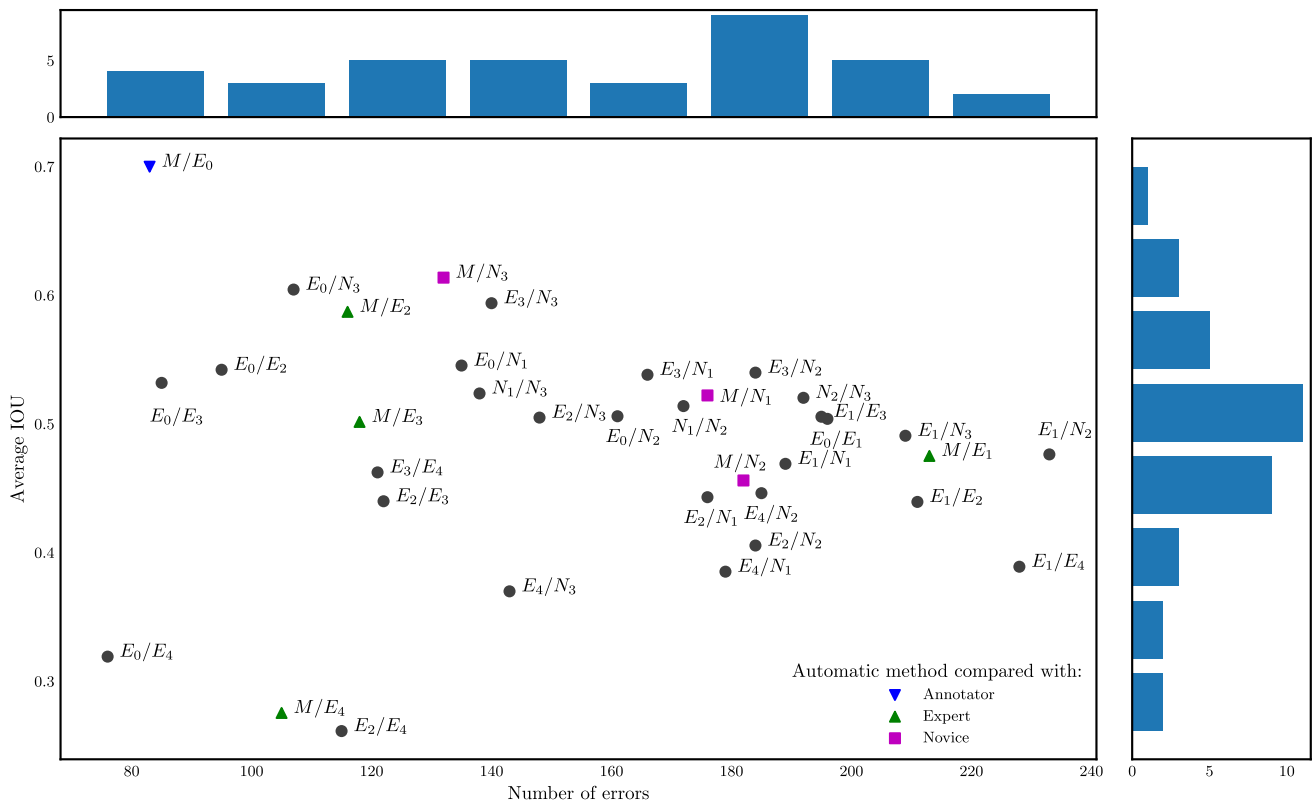


Fig. 2 Pairwise agreement between annotators in terms of the number of errors $e_{aa'}$ (horizontally) and $\text{IoU}_{aa'}$ (vertically). Best agreement corresponds to the top left corner. The comparison with the automatic

method is shown as color symbols, the comparison between human annotators is shown in black. Marginal histograms of $e_{aa'}$ and $\text{IoU}_{aa'}$ are shown at the top and right, respectively

Table 3 The pairwise differences in $IoU_{aa'}$ (above diagonal) and $e_{aa'}$ (below diagonal) for all pairs of annotators on the test dataset D_1 , as well as the mean values of IoU_a and e_a in the last column and row, respectively, with best values in bold

	M	E_0	E_1	E_2	E_3	E_4	N_1	N_2	N_3	IoU_a
M	•	0.7	0.48	0.6	0.51	0.27	0.52	0.45	0.62	0.52
E_0	89	•	0.49	0.5	0.53	0.32	0.52	0.52	0.62	0.53
E_1	221	209	•	0.44	0.51	0.39	0.47	0.48	0.49	0.47
E_2	120	148	211	•	0.44	0.26	0.44	0.41	0.5	0.45
E_3	132	85	195	122	•	0.46	0.54	0.54	0.59	0.52
E_4	111	76	228	115	121	•	0.39	0.45	0.37	0.36
N_1	186	138	189	176	166	179	•	0.51	0.52	0.49
N_2	184	192	233	184	184	185	172	•	0.52	0.48
N_3	134	134	209	148	140	143	138	192	•	0.53
e_a	147.1	133.9	211.9	153.0	143.1	144.8	168.0	190.8	154.8	•

200 lesions in a dataset D_1 containing 100 images. Out of 5 experts, the automatic method outperformed 2 in terms of e_a and 3 in terms of IoU_a .

The statistical significance (at level $\alpha = 0.05$ for all statistical tests) of pairwise differences between annotators according to the Wilcoxon test (“Significance of pairwise differences” section) is graphically displayed in Fig. 3. The automatic method M made significantly fewer errors than all the novices N and expert E_1 (Fig. 3, top). The number of errors made by M was also lower than that of E_2 , E_3 , and E_4 but not significantly so. In terms of the average IoU with respect to the experts (Fig. 3, bottom), the automatic method M was better than all other annotators except N_3 . However, the difference was significant only for E_2 and E_4 .

The number of errors and IoU averaged over all other experts is shown in Fig. 4. It can be seen that the automatic method M is among the best two methods in terms of IoU with a minimal difference and second to only E_0 in terms of the number of errors e .

Comparison with a consensus standard

Tables 4 and 5 present the outcome of comparisons with consensus standards, with and without expert E_1 (“Comparison with a consensus standard” section). In terms of the number of errors e , the automatic method M outperformed the novices N_1, N_2, N_3 and experts E_1, E_2, E_4 (Table 4). Excluding expert E_1 from the standards (Table 5), M outperformed all other annotators except E_0 . In terms of IoU, no method reached very high values (compare with Fig. 2), the automatic method M being slightly below average.

Comparison with the original annotator

Using the original annotator E_0 as a reference (“Comparison with the original annotator” section), the automatic method was the best in terms of IoU and second best after E_4 in

terms of the number of errors e (Table 6). The values of precision, recall and F_1 score for M were 0.78, 0.73 and 0.75, respectively.

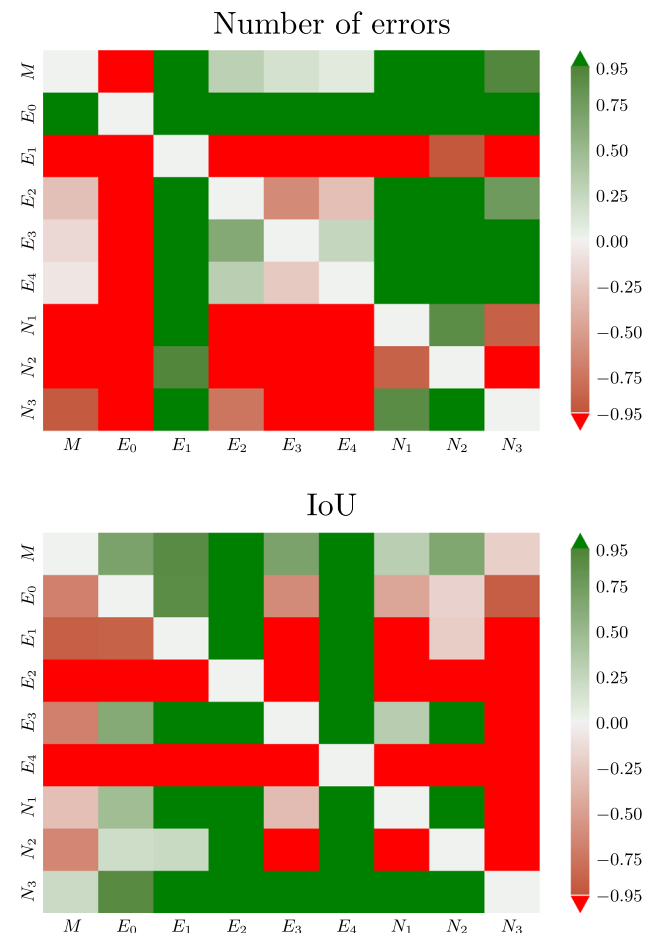


Fig. 3 The quantity $q = \pm(1 - p)$ from the Wilcoxon signed-rank test on the difference in the number of errors (top) and IoU (bottom) between an annotator and experts (see “Significance of pairwise differences” section). Green color (positive values) indicates that the row annotator is on the average closer to the experts than the column annotator and vice versa for red. Saturated green and red indicate statistically significant differences ($p < 0.05$)

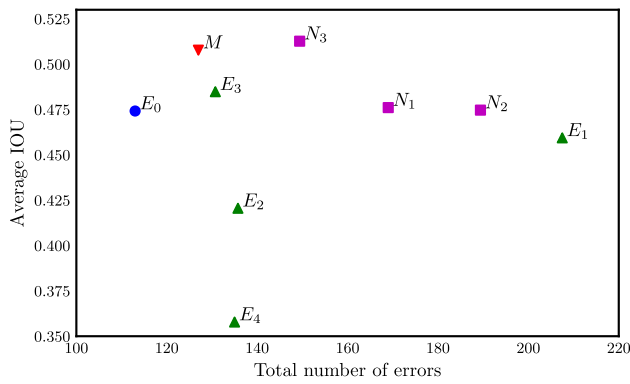


Fig. 4 Mean IoU_a and number of errors e_a for all anotators averaged over experts different from a . An ideal result would be in the top left

The statistical significance of the differences between annotators with respect to E_0 is shown in Fig. 5. The automatic method M significantly outperformed all novices N_1 , N_2 , and N_3 in terms of the number of errors e (Fig. 5, top). It also outperformed experts E_1 , E_2 and E_3 with the difference being significant only for E_1 . In terms of IoU, the automatic method M was significantly closer to E_0 than all other annotators (Fig. 5, bottom). This was expected, since M learnt from E_0 , but it nevertheless confirmed that the automatic method error is smaller than differences between experts.

Discussion

In this study, the best performing automatic caries detection method from the companion paper Part I [17] was validated by a comprehensive comparison with human annotators, specifically four highly experienced dentists (experts), three novices with less than five years of experience, and the original annotator who created the training dataset. The comparison was performed on an independent dataset of 100 bitewing radiographs, and while it was expected that

Table 5 IoU and number of errors for all annotators a with respect to a consensus standard, created as a majority consensus of experts excluding E_0 , E_1 and the expert being evaluated (shown by dashes)

a	$S_{3,4}$		$S_{2,4}$		$S_{2,3}$		Average	
	IoU	e	IoU	e	IoU	e	IoU	e
M	0.367	51	0.467	54	0.634	55	0.489	54
E_0	0.418	19	0.511	27	0.620	28	0.517	25
E_1	0.487	150	0.539	161	0.546	141	0.524	151
E_2	0.341	59	—	—	—	—	0.341	59
E_3	—	—	0.621	62	—	—	0.621	62
E_4	—	—	—	—	0.376	57	0.376	57
N_1	0.484	111	0.55	119	0.565	109	0.533	113
N_2	0.533	122	0.581	126	0.544	123	0.553	124
N_3	0.492	80	0.566	88	0.645	82	0.568	83

Best average values are shown in bold

the annotations by individual annotators would differ, the difference was surprisingly high (see “Methods” section, Table 1, Fig. 1). This demonstrated the difficulty of defining the ground truth for an objective comparison. In other comparable (i.e., in vivo) studies, the reported inter-rater agreement on evaluating bitewing radiographs ranged between $\kappa = 0.6$ in [19] to $\kappa = 0.8$ in [20] and was even as low as $\kappa = 0.246$ [16]. (Please note that this study formulates the task as a detection, not classification, so the absence of caries is not explicitly labeled and κ cannot be calculated.)

Since the ground truth was not available, it was impossible to accurately measure the diagnostic performance of the automatic method. Consequently, multiple complementary methods were used for the evaluation.

The first approach consisted of pairwise comparisons between all annotators (“Pairwise comparison” section), including the automatic method. It was evaluated how many of their annotations matched, and non-matching annotations were considered errors. In this aspect, the automatic method was significantly outperformed only by the original annotator

Table 4 IoU and number of errors for all annotators a with respect to a consensus standard, created as a majority consensus of experts excluding E_0 and the expert being evaluated (shown by dashes)

a	$S_{2,3,4}$		$S_{1,3,4}$		$S_{1,2,4}$		$S_{1,2,3}$		Average	
	IoU	e	IoU	e	IoU	e	IoU	E	IoU	e
M	0.492	64	0.423	78	0.484	71	0.580	80	0.495	73
E_0	0.519	27	0.469	54	0.519	44	0.587	52	0.524	44
E_1	0.530	136	—	—	—	—	—	—	0.530	136
E_2	—	—	0.382	84	—	—	—	—	0.382	84
E_3	—	—	—	—	0.595	59	—	—	0.595	59
E_4	—	—	—	—	—	—	0.390	90	0.390	90
N_1	0.557	101	0.526	82	0.548	74	0.559	81	0.547	85
N_2	0.573	122	0.557	117	0.556	106	0.534	114	0.555	115
N_3	0.580	78	0.519	78	0.548	71	0.603	80	0.563	77

Best average values are shown in bold

Table 6 Mean IoU and number of errors on the test dataset D_1 with respect to expert E_0

Measure	M	E_1	E_2	E_3	E_4	N_1	N_2	N_3
IoU	0.523	0.391	0.363	0.397	0.228	0.423	0.371	0.46
e	83	196	95	85	76	135	161	107

Best values marked in bold

(see Fig. 3, top). The mean intersection over union (IoU, i.e., overlap) was generally low, the automatic method ranked among the best with IoU=0.52 (Table 1, Fig. 3, bottom).

However, pairwise comparisons have limitations, as they evaluate agreement rather than correctness. Therefore, the second approach was based on creating a consensus standard of the experts (“Comparison with a consensus standard” section), considering only lesions on which the majority of experts agreed. The automatic method was outperformed

only by 2 of the 5 experts in terms of the number of errors (Table 4). The overlap (IoU) was again generally low for all annotators but the differences are probably not very meaningful, as the ability to detect caries in bitewing radiographs is clinically more important than slight variations in lesion size. The automatic method M was below average in terms of IoU. On the one hand, it was outperformed by the novices, on the other hand, some of the experts performed worse than M . This indicates the need to discuss a suitable IoU threshold for future studies on caries detection using deep learning. Note however, that our reported IoU are only calculated from matching annotations (as defined in “Pairwise comparison” section).

Finally, all annotators were compared with the original annotator E_0 (“Comparison with the original annotator” section). While this creates some advantage for the automatic method M that learnt from E_0 , such biased approach is common in machine learning studies. The ground truth used for comparison with dentists is generally produced by the same expert(s) who have annotated the training dataset [13, 20, 21], only Bayrakdar et al. [22] invited two additional experts to annotate the test dataset. In this study, the automatic method made fewer errors than all dentists except E_3 , and it was the best in terms of the average IoU by a significant margin (Table 6), showing that it learnt the annotation style of E_0 well. Even so, there were 83 differences (errors) between M and E_0 on the dataset D_1 . This number may seem high but given that the average of 13 proximal surfaces per radiograph in the test dataset, the 83 errors correspond to a classification error of $83/(100 \cdot 13) = 6.4\%$. Moreover, only one of the experts achieved a smaller value. The detection performance corresponds to an F_1 score of 0.75 (“Comparison with the original annotator”) which is lower than $F_1 = 0.80$ on the training dataset D_0 [17]. This may have been caused by a slightly higher prevalence of caries in the D_1 dataset or an inconsistency of annotations of the expert E_0 , as D_1 was annotated approximately 6 months after D_0 .

It is also noteworthy that the datasets D_0 and D_1 contained radiographs acquired using several different intraoral X-ray machines and sensors. This increases both the variability of the dataset and the difficulty of correct detection for the automatic method, thus possibly decreasing the detection accuracy. On the other hand, a model trained on such data should generalize better and perform well also for other unseen variants of bitewings radiographs. Overall, the results

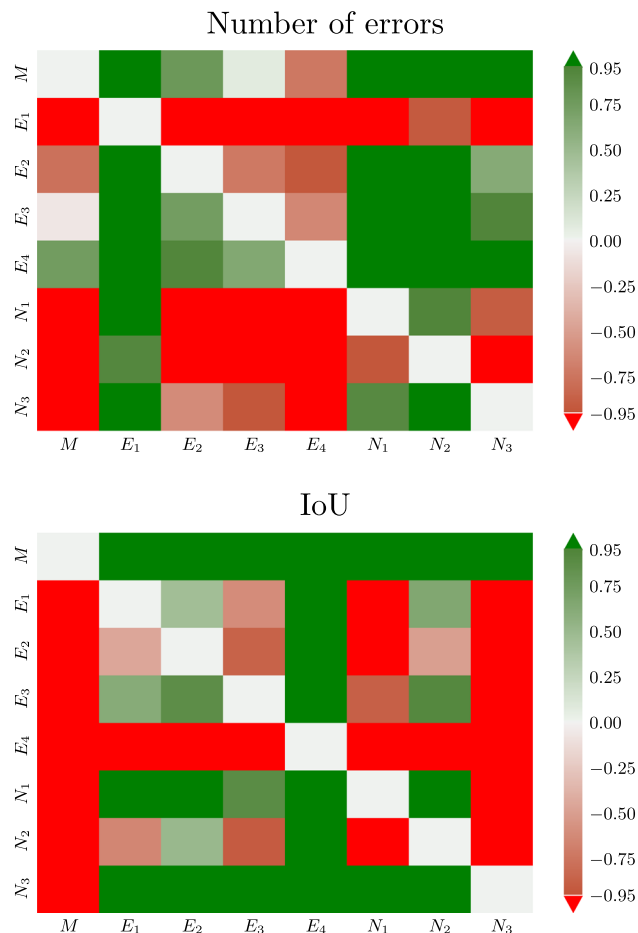


Fig. 5 The quantity $q = \pm(1 - p)$ from the Wilcoxon signed-rank test for the difference in the number of errors (top) and the IoU (bottom) between an annotator and expert E_0 on D_1 (see “Comparison with the original annotator” section). Green color (positive value) indicates that the row annotator is on the average closer to E_0 than the column annotator and vice versa for red. Saturated green and red indicate significant changes ($q > 0.95$ or $q < -0.95$, respectively)

of the automatic model were fully comparable with experienced dentists. It seems that further improvement will require a new approach to determine a reliable ground truth.

Conclusions

Repeatable and accurate caries detection in bitewing radiographs is challenging even for experienced dentists, which was confirmed by the marked differences between expert annotators. The tested automatic method consistently outperformed novices, and its performance was similar or superior to highly experienced experts. The presented method could therefore provide a useful second opinion for dentists, especially those with limited clinical experience, and help in improving both the accuracy and repeatability of caries detection.

Author Contributions A.T.: conceptualization, data curation and annotation, writing and editing. L.K.: implementation, experiments, writing and editing. V.N.: data validation and annotation, writing and editing. J.K.: image analysis, machine learning and statistical methodology, supervision of the implementation and experiments, writing and editing.

Funding Open access publishing supported by the National Technical Library in Prague. This work was supported by the General University Hospital in Prague (project GIP-21-SL-01-232) and by the OP VVV funded project CZ.02.1.01/0.0/0.0/16_019/0000765 “Research Center for Informatics.” The study sponsors had no involvement in the study design, analysis, interpretation of the data, writing, or choosing the publication venue.

Declarations

Ethics approval and consent to participate This research was approved by the Ethics Committee of the General University Hospital in Prague, protocol number 82/21. The patients signed a written informed consent, agreeing with the use of their data in anonymized form for research purposes.

Conflict of interest The authors declare no competing interests.

Open Access This article is licensed under a Creative Commons Attribution 4.0 International License, which permits use, sharing, adaptation, distribution and reproduction in any medium or format, as long as you give appropriate credit to the original author(s) and the source, provide a link to the Creative Commons licence, and indicate if changes were made. The images or other third party material in this article are included in the article’s Creative Commons licence, unless indicated otherwise in a credit line to the material. If material is not included in the article’s Creative Commons licence and your intended use is not permitted by statutory regulation or exceeds the permitted use, you will need to obtain permission directly from the copyright holder. To view a copy of this licence, visit <http://creativecommons.org/licenses/by/4.0/>.

References

- Kassebaum NJ, Bernabé E, Dahiya M, Bhandari B, Murray CJL, Marcenes W (2015) Global burden of untreated caries: a systematic review and meta-regression. *J Dent Res* 94(5):650–658. <https://doi.org/10.1177/0022034515573272>
- James SL, Abate D et al (2018) Global, regional, and national incidence, prevalence, and years lived with disability for 354 diseases and injuries for 195 countries and territories, 1990–2017: a systematic analysis for the global burden of disease study 2017. *The Lancet* 392(10159):1789–18580. [https://doi.org/10.1016/s0140-6736\(18\)32279-7](https://doi.org/10.1016/s0140-6736(18)32279-7)
- Rindal DB, Gordan VV, Litaker MS, Bader JD, Fellows JL, Qvist V, Wallace-Dawson MC, Anderson ML, Gilbert GH (2010) Methods dentists use to diagnose primary caries lesions prior to restorative treatment: findings from the dental pbrn. *J Dent* 38(12):1027–1032. <https://doi.org/10.1016/j.jdent.2010.09.003>
- Karlsson L (2010) Caries detection methods based on changes in optical properties between healthy and carious tissue. *Int J Dent* 270729. <https://doi.org/10.1155/2010/270729>
- Bader JD, Shugars DA, Bonito AJ (2001) Systematic reviews of selected dental caries diagnostic and management methods. *J Dent Educ* 65(10):960–968. <https://doi.org/10.1002/j.0022-0337.2001.65.10.tb03470.x>
- Gomez J (2015) Detection and diagnosis of the early caries lesion. *BMC Oral health* 15(S3). <https://doi.org/10.1186/1472-6831-15-S1-S3>
- Schwendicke F, Tzschoppe M, Paris S (2015) Radiographic caries detection: a systematic review and meta-analysis. *J Dent* 43(8):924–933. <https://doi.org/10.1016/j.jdent.2015.02.009>
- Pretty IA (2006) Caries detection and diagnosis: novel technologies. *J Dent* 34(10):727–739. <https://doi.org/10.1016/j.jdent.2006.06.001>
- Mohammad-Rahimi H, Motamedian SR, Rohban MH, Krois J, Uribe SE, Mahmoudinia E, Rokhshad R, Nadimi M, Schwendicke F (2022) Deep learning for caries detection: a systematic review. *J Dent* 122:104115. <https://doi.org/10.1016/j.jdent.2022.104115>
- Kamburoğlu K, Kolsuz E, Murat S, Yüksel S, Özen T (2012) Proximal caries detection accuracy using intraoral bitewing radiography, extraoral bitewing radiography and panoramic radiography. *Dentomaxillofacial Radiol* 41:450–459. <https://doi.org/10.1259/dmfr/30526171>
- Abdinian M, Razavi SM, Faghihian R, Samety AA, Faghihian E (2015) Accuracy of digital bitewing radiography versus different views of digital panoramic radiography for detection of proximal caries. *J Dent (Tehran)* 12(4):290–297
- Prados-Privado M, Villalón JG, Martínez-Martínez CH, Ivorra C, Prados-Frutos JC (2020) Dental caries diagnosis and detection using neural networks: a systematic review. *J Clin Med* 9(11):3579. <https://doi.org/10.3390/jcm9113579>
- Srivastava MM, Kumar P, Pradhan L, Varadarajan S (2017) Detection of tooth caries in bitewing radiographs using deep learning. In: NIPS workshop on machine learning for health, vol abs/1711.07312. <https://doi.org/10.48550/arXiv.1711.07312>
- Kumar P, Srivastava MM (2018) Example mining for incremental learning in medical imaging. In: IEEE symposium series on computational intelligence (SSCI). arXiv, ??? <https://doi.org/10.1109/SSCI.2018.8628895>
- García-Cañas A, Bonfanti-Gris M, Paraíso-Medina S, Martínez-Rus F, Pradies G (2022) Diagnosis of interproximal caries lesions in bitewing radiographs using a deep convolutional neural network-based software. *Caries Res* 56(5–6):503–511. <https://doi.org/10.1159/000527491>
- Natto ZS, Olwi A, Abduljawad F (2023) A comparison of the horizontal and vertical bitewing images in detecting approximal caries and interdental bone loss in posterior teeth: a diagnostic accuracy randomized cross over clinical trial. *J Dent Sci* 18:645–651. <https://doi.org/10.1016/j.jds.2022.08.006>
- Kunt L, Kybic J, Nagyová V, Tichý A (2023) Automatic caries detection in bitewing radiographs. part I: deep learning. Clin-

- ical Oral Investigation (27):7463–7471. <https://doi.org/10.1007/s00784-023-05335-1>
18. Tichý A, Kunt L, Kybic J (2023) Dental caries in bitewing radiographs. Mendeley Data. <https://doi.org/10.17632/4fbdxs7s7w.1>
 19. Estai M, Tennant M, Gebauer D, Vignarajan J, Mehdizadeh M, Saha S (2023) Evaluation of a deep learning system for automatic detection of proximal surface dental caries on bitewing radiographs. *Oral Surg Oral Med Oral Pathol Oral Radiol* 134(2):262–270. <https://doi.org/10.1016/j.oooo.2022.03.008>
 20. Chen X, Guo J, Ye J, Zhang M, Liang Y (2023) Detection of proximal caries lesions on bitewing radiographs using deep learning method. *Caries Res* 56(5–6):455–463. <https://doi.org/10.1159/000527418>
 21. Cantu AG, Gehrung S, Krois J, Chaurasia A, Rossi JG, Gaudin R, Elhennawy K, Schwendicke F (2020) Detecting caries lesions of different radiographic extension on bitewings using deep learning. *J Dent* 100:103425. <https://doi.org/10.1016/j.jdent.2020.103425>
 22. Bayrakdar IS, Orhan K, Akarsu S, Çelik O, Atasoy S, Pekince A, Yasa Y, Bilgir E, Sağlam H, Aslan AF, Odabaş A (2021) Deep-learning approach for caries detection and segmentation on dental bitewing radiographs. *Oral Radiology* 38(4). <https://doi.org/10.1007/s11282-021-00577-9>

Publisher's Note Springer Nature remains neutral with regard to jurisdictional claims in published maps and institutional affiliations.